Continuous defects: dislocations and disclinations in finite elasto-plasticity with initial dislocations heterogeneities

Raisa PASCAN*[,1], Sanda CLEJA-TIGOIU[2]

*Corresponding author
*[,1]"POLITEHNICA" University of Bucharest, Faculty of Applied Sciences
Splaiul Independenţei 313, 060042, Bucharest, Romania
pascanraisa@yahoo.com
[2]University of Bucharest, Faculty of Mathematics and Computer Science
Academiei 14, 010014, Bucharest, Romania
tigoiu@fmi.unibuc.ro

DOI: 10.13111/2066-8201.2015.7.4.15

Received: 10 October 2015 / Accepted: 10 November 2015

The 36th "Caius Iacob" Conference on Fluid Mechanics and its Technical Applications
29 - 30 October, 2015, Bucharest, Romania, (held at INCAS, B-dul Iuliu Maniu 220, sector 6)
Section 3. Equations of Mathematical Physics

Abstract: *Within the constitutive framework of second order plasticity, following [4,5], under the assumptions that the plastic distortion is not compatible, and the plastic connection is not compatible with the plastic distortion and has metric property, we define the lattice defects in crystalline elasto-plastic materials. The curl of plastic distortion, which defines the Burgers vector, is a measure of the dislocations. The disclination is characterized in terms of the second order tensor, which enters the expression of the plastic connection and generates the Frank vector. The free energy density is postulated to be dependent on the elastic deformation and the measures of the defects. The non-local, diffusion-type evolution equations for plastic distortion and the damage tensor are derived to be compatible with the dissipation inequality, while the micro stress momenta, associated with the plastic and disclination mechanisms, are derived from the free energy function. We restrict the evolution equations for defects to small elastic and plastic distortions, considered to be wedge disclinations and edge dislocations. The finite element method is applied to numerically study the evolution of the defects, when the initial dislocation heterogeneities are considered.*

Key Words: *Burgers vector; dislocation density; disclination density; dipole of disclinations; diffusion-like evolution for plastic distortion; variational equality; FEM and update algorithm.*

1. INTRODUCTION

Unlike [8] where the scalar densities of dislocations in slip systems have been considered, and to [6,7] where the tensorial densities of dislocations have been also introduced, the present model involves the tensorial densities of dislocations and disclinations. We mention the theory of dislocation and disclination fields developed in [11,15] within the small elasto-plastic distortions as being closed to our model. Experimental observation of the continuous defects like dislocations and disclinations have been observed within transmission – electron

– microscopy, see for instance [2]. The defect densities are related to the incompatibility of the plastic distortion, $\mathbf{F}^p$ which is not a gradient, i.e. the dislocation density, and the incompatibility of the plastic connection, which involves the disclination tensor, $\boldsymbol{\Lambda}$, and has a non zero curvature, i.e. the disclination density. The defect densities characterize the Burgers and Frank vectors defined within the finite deformation framework being reduced to $\mathrm{curl}\mathbf{H}^p$ and $\mathrm{curl}\boldsymbol{\Lambda}$ in the case of small distortions.

In the present paper we consider the constitutive framework developed in paper [10], where both type of defects: dislocations and disclinations are considered and the free energy density is formulated like in [5] (following the idea of Gurtin [12,13]). The reduced dissipation inequality allows us to introduce the viscoplastic-like equations for micro forces and derive the appropriate non-local evolution diffusion-like equations for the plastic distortion and for the disclination tensor. In paper [10] we derived the non-local diffusion like evolution equations for wedge disclinations and edge dislocations (as a part case of the general developed theory therein). In [8,9] non-local diffusion-type equations for scalar densities of dislocations were represented.

In the present paper we considered the model of edge dislocations coupled with wedge disclinations in the case of small elasto-plastic distortions. We numerically solved the initial and boundary value problem. We considered a tensile problem in a rectangular sheet when the initial heterogeneity of the defects was prescribed by the dislocation tensor able to induce the dipole of disclinations in the process. We emphasized the dislocation-disclination interaction and the diffusion effects on the material behavior.

In paper [10] the problem of the disclination-dislocation interplay was studied under the hypothesis that the initial heterogeneity of the defects was prescribed in term of disclination tensor $\boldsymbol{\Lambda}$.

The initial and boundary value problem is formulated as follows: Find the displacement vector $\mathbf{u}$, the plastic distortion $\mathbf{H}^p$ and the disclination tensor $\boldsymbol{\Lambda}$, as time dependent functions defined on the domain occupied by the body, which satisfy the equilibrium equation and evolution equations for $\mathbf{H}^p$ and $\boldsymbol{\Lambda}$.

The corresponding variational equalities for the incremental equilibrium equation and for the evolution equations for the plastic distortion and for the disclination tensor were formulated. The discretization of the weak forms for the evolution equations are obtained by using the Crank-Nicolson method.

Notations: For a second-order tensor $\mathbf{A} \in \mathrm{Lin}$ we denote: $\left(\nabla\mathbf{A}\right)_{ijk} = \dfrac{\partial A_{ij}}{\partial X^k}$ the gradient components of the field $\mathbf{A}$; $\mathrm{curl}\mathbf{A}$ is defined by $(\mathrm{curl}\mathbf{A})_{pi} = \in_{ijk} \dfrac{\partial A_{pk}}{\partial X^j}$, where $\in_{ijk}$ denote Ricci permutation tensor components; $\left\{\mathbf{A}\right\}^S$, $\left\{\mathbf{A}\right\}^a$ are the symmetric and skew-symmetric parts of $\mathbf{A}$.

2. CONSTITUTIVE FRAMEWORK

The tensorial measure of the defects will be the disclination tensor $\boldsymbol{\Lambda}$ and the dislocation tensor $\boldsymbol{\alpha} = \mathrm{curl}\mathbf{H}^p$, both of them second order tensor fields dependent on material particle and time. The disclination tensor $\boldsymbol{\Lambda}$, generates the non-zero curvature of the so-called plastic connection and measures the discrepancy between the plastic connection and Bilby type plastic connection, $\overset{(p)}{\mathcal{A}}$, [3] which is compatible with the plastic distortion, namely $\overset{(p)}{\mathcal{A}} \equiv (\mathbf{F}^p)^{-1}\nabla\mathbf{F}^p$. The models involve the multiplicative decomposition of the deformation gradient $\mathbf{F}$ in the elastic and plastic distortions, $\mathbf{F} = \mathbf{F}^e\mathbf{F}^p$. The free energy imbalance principle describes the dissipative nature of the defects such as dislocations and disclinations. In the model considered here we assume that the free energy density ψ in the reference configuration is given by

$$\psi = \frac{1}{2}\mathcal{E}(\mathbf{C}-\mathbf{C}^p)\cdot(\mathbf{C}-\mathbf{C}^p) + \frac{1}{2}\beta_2\mathbf{S}^p\cdot\mathbf{S}^p + \frac{1}{2}\beta_3\mathbf{\Lambda}\cdot\mathbf{\Lambda} + \frac{1}{2}\beta_4\nabla\mathbf{\Lambda}\cdot\nabla\mathbf{\Lambda}, \tag{1}$$

where $\mathcal{E}$ is the elastic stiffness tensor. The following notations were introduced

$$\begin{aligned} &\mathbf{C} = (\mathbf{F})^T\mathbf{F},\ \mathbf{C}^p = (\mathbf{F}^p)^T\mathbf{F}^p,\quad (\mathbf{S}^p\mathbf{v})\mathbf{u} \equiv \mathcal{N}^p(\mathbf{u}\times\mathbf{v}) \quad \forall\, \mathbf{u},\mathbf{v} \ \text{vectors},\\ &\text{with } \mathcal{N}^p = (\mathbf{F}^p)^{-1}\text{curl}\mathbf{F}^p + (\mathbf{C}^p)^{-1}\big((\text{tr}\,\mathbf{\Lambda})\mathbf{I} - (\mathbf{\Lambda})^T\big). \end{aligned} \tag{2}$$

Here the second order torsion tensor is denoted by, $\mathcal{N}^p$, and is associated with the Cartan torsion $\mathbf{S}^p$, a third order tensor.

We introduce a tensorial measure of dislocations as: $\boldsymbol{\alpha} = \left(\mathbf{F}^p\right)^{-1}\text{curl}\mathbf{F}^p$.

Within the finite deformation elasto-plastic framework the non-local evolution equations for plastic distortion and disclination tensor were derived to be compatible with the dissipation inequality, corresponding to the adopted expressions of the free energy density.

Here we restrict ourselves to the case of small elastic and plastic distortions. The linearized expressions for the finite deformation fields are given by

$$\begin{aligned} &\mathbf{F} \cong \mathbf{I} + \mathbf{H},\quad |\,\mathbf{H}| << 1,\quad \mathbf{H} = \nabla\mathbf{u},\quad \boldsymbol{\varepsilon} = \{\mathbf{H}\}^S,\\ &\mathbf{F}^p = \mathbf{I} + \mathbf{H}^p,\quad |\,\mathbf{H}| << 1,\quad \overset{(p)}{\mathcal{A}} \cong \nabla\mathbf{H}^p,\quad \boldsymbol{\varepsilon}^p = \{\mathbf{H}^p\}^S,\\ &\mathbf{C} - \mathbf{C}^p = 2(\boldsymbol{\varepsilon} - \boldsymbol{\varepsilon}^p),\quad \mathbf{C}^p = \mathbf{I} + 2\boldsymbol{\varepsilon}^p, \end{aligned} \tag{3}$$

where $\mathbf{u}$ is the displacement vector. The Cartan torsion $\mathbf{S}^p$, and the second order, $\mathcal{N}^p$, are given by

$$\begin{aligned} &\mathbf{S}^p = Skw\nabla\mathbf{H}^p + Skw(\mathbf{\Lambda}\times\mathbf{I}),\\ &\mathcal{N}^p = \text{curl}\mathbf{H}^p + \big((\text{tr}\,\mathbf{\Lambda})\mathbf{I} - (\mathbf{\Lambda})^T\big). \end{aligned} \tag{4}$$

The influence of defects is described by the presence of the dislocation density, $\boldsymbol{\alpha} = \text{curl}\mathbf{H}^p$, and the disclination tensor, $\mathbf{\Lambda}$, with the mention that $\text{curl}\mathbf{H}^p$ and $\mathbf{\Lambda}$ are independent terms in (4) and have the same order of magnitude.

The Cauchy stress tensor is given by the formulae $\frac{1}{\hat{\rho}}\{\mathbf{T}\}^S = 2\mathbf{F}\mathcal{E}\left(\mathbf{C}-\mathbf{C}^p\right)\mathbf{F}^T$, and in the case of small distortions it takes the following form: $\frac{1}{\hat{\rho}}\mathbf{T} = \mathcal{E}\left(\boldsymbol{\varepsilon}-\boldsymbol{\varepsilon}^p\right)$. $\hat{\rho}$ represents the mass density in the current configuration.

3. WEDGE DISCLINATIONS AND EDGE DISLOCATIONS

We recall that a wedge disclination is developed within the body if $(\text{curl}\boldsymbol{\Lambda})\mathbf{e}_3 \parallel \mathbf{e}_3$. We consider that $\Lambda_{3s} = \Lambda_{3s}(x^1, x^2),\ s = 1, 2$ are non-vanishing only, and $\text{curl}\boldsymbol{\Lambda} := \left(\frac{\partial \Lambda_{32}}{\partial x^1} - \frac{\partial \Lambda_{31}}{\partial x^2}\right)\mathbf{e}_3 \otimes \mathbf{e}_3$. The edge dislocation, which generates a Burgers vector in the plane, is characterized by the plastic components H_{ij}^p with $i, j = 1, 2,$ being function of $(x^1, x^2),$ and

$$\text{curl}\mathbf{H}^p = \left(\frac{\partial H_{12}^p}{\partial x^1} - \frac{\partial H_{11}^p}{\partial x^2}\right)\mathbf{e}_1 \otimes \mathbf{e}_3 + \left(\frac{\partial H_{22}^p}{\partial x^1} - \frac{\partial H_{21}^p}{\partial x^2}\right)\mathbf{e}_2 \otimes \mathbf{e}_3. \tag{5}$$

The evolution equations for the plastic distortion and the disclination tensor were derived in [10] and take the following form:

Proposition The fields $\mathbf{H}^p$ and $\boldsymbol{\Lambda}$ are described by the following evolution equations

$$\begin{aligned}
&\xi_1 \dot{\mathbf{H}}^p = -\beta_2\, \text{curl}(\,\text{curl}\mathbf{H}^p) + \beta_2 curl(\boldsymbol{\Lambda}^T) + \mathbf{T} + \\
&\qquad + 4\beta_2\, \boldsymbol{\Lambda}^T \boldsymbol{\Lambda} - 2\beta_2 \left(\boldsymbol{\Lambda}^T\, (curl\mathbf{H}^p)^T + (\,curl\mathbf{H}^p)\boldsymbol{\Lambda}\right) \\
&\xi_2\, \dot{\boldsymbol{\Lambda}} = \beta_4 \Delta\boldsymbol{\Lambda} - (\beta_3 + 2\beta_2)\boldsymbol{\Lambda} + 2\beta_2\, (curl\mathbf{H}^p)^T - \beta_4 \frac{\partial \Lambda_{3s}}{\partial x^k}\frac{\partial H_{qs}^p}{\partial x^k}\mathbf{e}_3 \otimes \mathbf{e}_q - \\
&\qquad - \beta_4 \frac{\partial \Lambda_{3q}}{\partial x^k}\frac{\partial(\text{tr}\mathbf{H}^p)}{\partial x^k}\mathbf{e}_3 \otimes \mathbf{e}_q, \quad \forall\, s, q, k \in \{1, 2\}
\end{aligned} \tag{6}$$

PROBLEM. Solve the quasi-static, initial and boundary value problems associated to the incremental equilibrium equation $div\left(\mathcal{E}(\dot{\boldsymbol{\varepsilon}} - \dot{\boldsymbol{\varepsilon}}^p)\right) = 0$ and coupled with the flow rules (6).

The variational problem, which defines the velocity field at time, t, is numerically solved by finite element method, and the current state in the sheet is defined via an update algorithm connected with the non-local evolution equations (6).

In our example it is assumed that the initial existing defects inside the microstructure are reduced to an area of dislocations, which is characterized by the dislocation tensor $\boldsymbol{\alpha}^0(\mathbf{x})$. In the formulated boundary problem defining the initial conditions for $\mathbf{H}^p(\mathbf{x})$ is essential. We follow the procedure proposed by [1] and [15]:

$$\text{curl}\mathbf{H}_0^p = \boldsymbol{\alpha}^0, \quad \text{div}\mathbf{H}_0^p = 0, \quad \forall \mathbf{x} \in \Omega, \quad \mathbf{H}_0^p = \mathbf{0}, \quad \forall \mathbf{x} \in \partial\Omega. \tag{7}$$

This means that the following **problems** has to be satisfied by $H_{ij}^p,\ i, j \in \{1, 2\}$, respectively

$$\begin{aligned}
&\Delta H_{11}^p = -\alpha_{13,2}^0 \ \ \forall \mathbf{x} \in \Omega, \quad H_{11}^p = 0,\ \forall \mathbf{x} \in \partial\Omega; \ \ \Delta H_{12}^p = \alpha_{13,1}^0 \ \ \forall \mathbf{x} \in \Omega, \ \ H_{12}^p = 0, \ \forall \mathbf{x} \in \partial\Omega; \\
&\Delta H_{21}^p = -\alpha_{23,2}^0 \ \ \forall \mathbf{x} \in \Omega, \quad H_{21}^p = 0,\ \forall \mathbf{x} \in \partial\Omega; \ \ \Delta H_{22}^p = \alpha_{23,1}^0 \ \ \forall \mathbf{x} \in \Omega, \ \ H_{22}^p = 0, \ \forall \mathbf{x} \in \partial\Omega.
\end{aligned} \tag{8}$$

In order to build a rotation with opposites signs in Burgers vector at the initial time (see Fig. 8) we consider $\text{curl}\boldsymbol{\alpha}_0^T = g(\mathbf{x})$.

The function $g(\mathbf{x})$ is defined by the formulae

$$g(x_1,x_2)=\begin{cases} g_{\max}\exp[-k(\dfrac{(x_1-x_0^{sup})^2}{a_x^2}+\dfrac{(x_2-y_0^{sup})^2}{a_y^2})], & (x_1,x_2)\in\Omega_1 \\ -g_{\max}\exp[-k(\dfrac{(x_1-x_0^{\inf})^2}{a_x^2}+\dfrac{(x_2-y_0^{\inf})^2}{a_y^2})], & (x_1,x_2)\in\Omega_2 \\ 0,\ (x_1,x_2)\in\Omega\setminus(\Omega_1\cup\Omega_2), & \end{cases} \tag{9}$$

where Ω_1,Ω_2 are two open disjoints sets:

$$\Omega_1=\left\{(x_1,x_2)/(x_1-x_0^{sup})^2/a_x^2+(x_2-y_0^{sup})^2/a_y^2\le 1\right\},$$

$$\Omega_2=\left\{(x_1,x_2)/(x_1-x_0^{\inf})^2/a_x^2+(x_2-y_0^{\inf})^2/a_y^2\le 1\right\}.$$

To find the initial condition for the dislocation tensor $\boldsymbol{\alpha}^0$ we solve the following problem:

$$\mathrm{div}\boldsymbol{\alpha}_0^T=0,\ \ \mathrm{curl}\boldsymbol{\alpha}_0^T=g(\mathbf{x}),\ \ \forall\mathbf{x}\in\Omega,\quad \boldsymbol{\alpha}^0=\mathbf{0},\quad \forall\mathbf{x}\in\partial\Omega. \tag{10}$$

Equivalently the following problems have to be solved for unknowns $\alpha_{13}^0,\alpha_{23}^0$:

$$\Delta\alpha_{13}^0=-g_{,2}\ \ \forall\mathbf{x}\in\Omega,\quad \alpha_{13}^0=0,\ \forall\mathbf{x}\in\partial\Omega;\ \ \Delta\alpha_{23}^0=g_{,1}\ \ \forall\mathbf{x}\in\Omega,\quad \alpha_{23}^0=0,\ \forall\mathbf{x}\in\partial\Omega. \tag{11}$$

4. THE WEAK FORMULATION IN THE CASE OF SMALL DISTORTIONS

The weak form of the evolution equation written above can be characterized for any pairs $(\mathbf{G},\boldsymbol{\Psi})$

$$\begin{aligned}\int_\Omega \xi_1\dot{\mathbf{H}}^p\cdot\mathbf{G}\mathrm{d}\mathbf{x}=&-\int_\Omega\beta_2\ (\mathrm{curl}\mathbf{H}^p)\cdot(\mathrm{curl}\mathbf{G})\mathrm{d}\mathbf{x}+\int_{\partial\Omega}\beta_2(\mathrm{curl}\mathbf{H}^p)\,(\boldsymbol{\epsilon}\,\mathbf{n})\cdot\mathbf{G}\mathrm{d}s+\\ &+\int_\Omega\left\{\beta_2 curl(\boldsymbol{\Lambda}^T)+\mathbf{T}+4\beta_2\ \boldsymbol{\Lambda}^T\boldsymbol{\Lambda}\right\}\cdot\mathbf{G}\mathrm{d}\mathbf{x}-\\ &-2\int_\Omega\beta_2\left(\boldsymbol{\Lambda}^T\ (curl\mathbf{H}^p)^T+(\ curl\mathbf{H}^p)\boldsymbol{\Lambda}\right)\cdot\mathbf{G}\mathrm{d}\mathbf{x}\end{aligned} \tag{12}$$

$$\begin{aligned}\int_\Omega\xi_2\dot{\boldsymbol{\Lambda}}\cdot\boldsymbol{\Psi}\mathrm{d}x=&-\int_\Omega\beta_4\nabla\boldsymbol{\Lambda}\cdot\nabla\boldsymbol{\Psi}\mathrm{d}\mathbf{x}+\int_{\partial\Omega}\beta_4(\nabla\boldsymbol{\Lambda})\mathbf{n}\cdot\boldsymbol{\Psi}\mathrm{d}s-\\ &-\int_\Omega\left\{(\beta_3+2\beta_2)\boldsymbol{\Lambda}+2\beta_2\ (curl\mathbf{H}^p)^T\right\}\cdot\boldsymbol{\Psi}\mathrm{d}\mathbf{x}-\\ &-\int_\Omega\left(\beta_4\frac{\partial\Lambda_{3s}}{\partial x^k}\frac{\partial H^p_{qs}}{\partial x^k}+\beta_4\frac{\partial\Lambda_{3q}}{\partial x^k}\frac{\partial(\mathrm{tr}\mathbf{H}^p)}{\partial x^k}\right)\mathbf{e}_3\otimes\mathbf{e}_q\cdot\boldsymbol{\Psi}\mathrm{d}\mathbf{x}\end{aligned} \tag{13}$$

In order to obtain a boundary value problem we attach the boundary condition for the incremental equilibrium equation, for the evolution equation for the plastic distortion and for the disclination tensor. Let Ω be the domain occupied by the body $\mathcal{B}$ at the moment t and $\Gamma=\partial\Omega$ be the boundary of Ω. We assume the following boundary conditions for the incremental equilibrium equation:

$$\dot{\mathbf{T}}\mathbf{n}=\dot{\mathbf{t}}\quad\text{on}\quad\Gamma_1,\quad \mathbf{v}=\mathbf{v}^*\quad\text{on}\quad\Gamma_2, \tag{14}$$

where $\Gamma_1\cup\Gamma_2=\Gamma$ and $\Gamma_1\cap\Gamma_2=\varnothing$, and for the evolution equation for the plastic distortion:

$$\boldsymbol{\alpha}\,(\boldsymbol{\epsilon}\,\mathbf{n}) = (\mathrm{curl}\mathbf{H}^p)\,(\boldsymbol{\epsilon}\,\mathbf{n}) = \mathbf{h}^p \quad \text{on} \quad \Gamma \tag{15}$$

For the evolution equation for the disclination tensor we considered the following boundary condition:

$$\left(\nabla\boldsymbol{\Lambda}\right)\mathbf{n} = \boldsymbol{\lambda} \;\; \text{on} \;\; \Gamma. \tag{16}$$

In the above conditions, $\mathbf{n}$ is the outward normal to the boundary of the domain Ω and $\boldsymbol{\epsilon}$ represents Ricci permutation tensor. The corresponding variational equality for the incremental equilibrium equation is given by:

$$\int_\Omega \left[\boldsymbol{\mathcal{E}}\left(\frac{1}{2}(\nabla\mathbf{v} + (\nabla\mathbf{v})^{\mathrm{T}}) - \{\dot{\mathbf{H}}^p\}^S \right)\right]\cdot\{\nabla\mathbf{w}\}^S\, \mathrm{d}\mathbf{x} - \int_{\Gamma_1} \dot{\mathbf{t}}\cdot\mathbf{w}\mathrm{d}s = 0, \quad \forall\mathbf{w}\in \mathrm{V}^0_{ad}. \tag{17}$$

The unknown $\mathbf{v}\in \mathrm{V}_{ad} = \left\{\mathbf{v}:\Omega\to\mathbf{R}^3 \,|\, \mathbf{v} = \mathbf{v}^* \text{ on } \Gamma_2\right\}$ and $\mathrm{V}^0_{ad} = \left\{\mathbf{w}:\Omega\to\mathbf{R}^3 \,|\, \mathbf{w} = \mathbf{0} \text{ on } \Gamma_2\right\}$.

4.1 The discretization of the weak form for the evolution equations

Let us consider $(t_n)_{1\le n\le N}$ a partition of the time interval $\left[0,T\right]$ and $\mathrm{d}t = t_{n+1} - t_n$ be the increment of time. Let Ω^n be the domain occupied by the body on the $\left[t_n, t_{n+1}\right]$ interval. For the discretization we apply the Crank-Nicolson method (see for instance [16]). The time derivative of the plastic distortion and of the disclination tensor are both approximated by formulas $\dot{\mathbf{H}}^p \approx \dfrac{\mathbf{H}^p_{n+1} - \mathbf{H}^p_n}{\mathrm{d}t}$ and $\dot{\boldsymbol{\Lambda}} \approx \dfrac{\boldsymbol{\Lambda}_{n+1} - \boldsymbol{\Lambda}_n}{\mathrm{d}t}$. We approximate the plastic distortion and the disclination tensor in linear terms, by $\mathbf{H}^p \approx \dfrac{\mathbf{H}^p_{n+1} + \mathbf{H}^p_n}{2}$, $\boldsymbol{\Lambda} \approx \dfrac{\boldsymbol{\Lambda}_{n+1} + \boldsymbol{\Lambda}_n}{2}$ and in nonlinear terms, by $\mathbf{H}^p \approx \mathbf{H}^p_{\bar{n}} = \dfrac{3}{2}\mathbf{H}^p_n - \dfrac{1}{2}\mathbf{H}^p_{n-1}$, $\boldsymbol{\Lambda} \approx \boldsymbol{\Lambda}_{\bar{n}} = \dfrac{3}{2}\boldsymbol{\Lambda}_n - \dfrac{1}{2}\boldsymbol{\Lambda}_{n-1}$.

With these considerations (in the $\mathbf{h}^p = 0, \boldsymbol{\lambda} = 0$ hypotheses) the discretization of the weak forms for the plastic distortion and for the disclination tensor becomes:

$$\begin{aligned}
&\int_\Omega \xi_1 \frac{\mathbf{H}^p_{n+1} - \mathbf{H}^p_n}{\mathrm{d}t}\cdot\mathbf{G}\mathrm{d}\mathbf{x} = -\int_\Omega \beta_2\, \mathrm{curl}\left(\frac{\mathbf{H}^p_{n+1} + \mathbf{H}^p_n}{2}\right)\cdot(\mathrm{curl}\mathbf{G})\mathrm{d}\mathbf{x} + \\
&+\int_\Omega \left\{ \beta_2 \mathrm{curl}\left(\frac{\boldsymbol{\Lambda}^T_{n+1} + \boldsymbol{\Lambda}^T_n}{2}\right) + \mathbf{T}_n + 4\beta_2\, \boldsymbol{\Lambda}^T_{\bar{n}}\, \frac{\boldsymbol{\Lambda}_{n+1} + \boldsymbol{\Lambda}_n}{2}\right\}\cdot\mathbf{G}\mathrm{d}\mathbf{x} - \\
&-2\int_\Omega \beta_2 \left\{ \boldsymbol{\Lambda}^T_{\bar{n}} \left(\mathrm{curl}\left(\frac{\mathbf{H}^p_{n+1} + \mathbf{H}^p_n}{2}\right)\right)^T + \mathrm{curl}\left(\frac{\mathbf{H}^p_{n+1} + \mathbf{H}^p_n}{2}\right)\boldsymbol{\Lambda}_{\bar{n}} \right\}\cdot\mathbf{G}\mathrm{d}\mathbf{x}
\end{aligned} \tag{18}$$

$$\begin{aligned}
&\int_{\Omega^n} \xi_2 \frac{\boldsymbol{\Lambda}_{n+1} - \boldsymbol{\Lambda}_n}{dt}\cdot\boldsymbol{\Psi}\mathrm{d}\mathbf{x} = -\int_{\Omega^n} \beta_4 \nabla\left(\frac{\boldsymbol{\Lambda}_{n+1} + \boldsymbol{\Lambda}_n}{2}\right)\cdot\nabla\boldsymbol{\Psi}\mathrm{d}\mathbf{x} - \\
&-\int_{\Omega^n} \left\{ (\beta_3 + 2\beta_2)\frac{\boldsymbol{\Lambda}_{n+1} + \boldsymbol{\Lambda}_n}{2} + 2\beta_2 \left(curl\left(\frac{\mathbf{H}^p_{n+1} + \mathbf{H}^p_n}{2}\right)\right)^T \right\}\cdot\boldsymbol{\Psi}\mathrm{d}\mathbf{x} - \\
&-\int_{\Omega^n} \left(\frac{\beta_4}{2}\frac{\partial(\Lambda^n_{3s} + \Lambda^{n+1}_{3s})}{\partial x^k}\frac{\partial(H^p_{qs})_{\bar{n}}}{\partial x^k} + \frac{\beta_4}{2}\frac{\partial(\Lambda^{n+1}_{3q} + \Lambda^n_{3q})}{\partial x^k}\frac{\partial(\mathrm{tr}\mathbf{H}^p_{\bar{n}})}{\partial x^k} \right)\mathbf{e}_3\otimes\mathbf{e}_q\cdot\boldsymbol{\Psi}\mathrm{d}\mathbf{x}
\end{aligned} \tag{19}$$

4.2 The discretization of the weak form for the incremental equilibrium equation type

In the same way we obtain the discretization for the variational equality (7):

$$\int_{\Omega_n}\left[\mathcal{E}\left(\frac{1}{2}(\nabla\mathbf{v}_n+(\nabla\mathbf{v}_n)^{\mathrm{T}})-\left\{\frac{\mathbf{H}^p_{n+1}-\mathbf{H}^p_n}{\mathrm{d}t}\right\}^S\right)\right]\cdot\{\nabla\mathbf{w}\}^S\,\mathrm{d}\mathbf{x}-\int_{\Gamma^1_n}\frac{\mathbf{t}_{n+1}-\mathbf{t}_n}{\mathrm{d}t}\cdot\mathbf{w}\mathrm{d}A=0 \qquad (20)$$

The **algorithm** for solving the system of the equations (20), (18) and (19): The elastic problem is resolved until the averaged value of the equivalent stress state becomes equal or larger than a critical value, i.e. $\int_{\Omega}\sqrt{\mathbf{T}'\cdot\mathbf{T}'}\mathrm{d}\mathbf{x}/\mathcal{A}(\Omega)<\sqrt{2/3}\sigma_y$. Assume that at time t_0 the stress reached the yield condition. We mention that $\mathcal{A}(\Omega)$ represents the area of the domain Ω.

At this moment we solve problems (8) together with (11) by employing the finite element method (FEM). The fields $H^p_{ij}(t_0)$, represent the initial conditions for the evolution equations (18) and (19). We consider no disclinations at the t_0 moment ($\Lambda_{31}(t_0)=\Lambda_{32}(t_0)=0$). For $t_n\geq t_0$

- We suppose that at the moment t_n one knows the current state of the body, namely: $\mathbf{H}^p_n,\mathbf{\Lambda}_n,\mathbf{v}_n$. Applying the Crank-Nicolson method (see [19]) we find the solutions for $\mathbf{H}^p,\mathbf{\Lambda}$ at the moment of time t_{n+1}, namely $\mathbf{H}^p_{n+1},\mathbf{\Lambda}_{n+1}$;
- We return at the discretisation of the weak form for equilibrium equation for the rate of displacement $\mathbf{v}$ and we find the solution at the moment of time t_{n+1}, namely $\mathbf{v}_{n+1}$.
- One can update the mesh and all the measures calculated on the previous mesh, knowing the velocity field $\mathbf{v}_{n+1}$. The procedure continues.

5. NUMERICAL SIMULATION

In the numerical simulations, a square domain, $\Omega=[0,L_0]^2$, $L_0=5\mathrm{nm}$, occupied by an aluminum crystal has been considered. In the tensile test, the edge $x_1=0$ (left side) is fixed. The rectangular sheet is subject to a displacement vector applied with a constant velocity on the right hand side of the plate. We suppose that the left-hand edge is not deformed in the x_1 − direction, but it can be freely deformed in the direction of x_2 - axis, while the other sides of the plate are free of stress. The edge $x_1=L_0$ (right side) is moved with a constant speed $v_1=5.0\times10^{-2}\,\mathrm{nm}/\mu\mathrm{s}$ applied along the axis Ox_1 and it can be freely deformed in the direction of x_2. The time integration step (time increment) $\mathrm{d}t=10^{-4}\mu\mathrm{s}$ generates an incremental elongation $\mathrm{d}\varepsilon_{11}=10^{-6}$.

The numerical algorithms were performed using the Finite Element Method, with the FreeFem++ programming environment [14]. The programme ParaView 4.0.1 has been used to plot the numerical results.

The procedures for the mesh refinement have been used in the zones with a maximum value intensity, allowing for the optimization of the number of FEs considered herein, at the same time increasing the computation speed.

The values of the **material parameters** for aluminum [12] are as follows: $\mu = 27{\cdot}10^3[\text{MPa}]$, $\nu = 0.3$, $\sigma_y = 70[\text{MPa}]$, $\mathcal{E}_{1111}=\mathcal{E}_{2222}=\dfrac{2\mu(1\text{-}\nu)}{1\text{-}2\nu}$, $\mathcal{E}_{1122}=\mathcal{E}_{2211}=\dfrac{2\mu\nu}{1\text{-}2\nu}$, $\mathcal{E}_{1221}=\mathcal{E}_{1212}=\mathcal{E}_{2112}=\mathcal{E}_{2121}=\mu$. The parameters appearing in the evolution equations are numerically evaluated in [10]: $\xi_1 = 5.7{\cdot}10^4[\mu\text{sMpa}]$, $\xi_2 = 1.7{\cdot}10^3\left[\mu\text{snm}^2\text{MPa}\right]$, $\beta_2 = 5.7{\cdot}10^3[\text{nm}^2\text{MPa}]$, $\beta_3 = \beta_2$, $\beta_4 = 75\left[nm^3\text{MPa}\right]$. The **geometrical parameters** which characterize the initial values of the dislocations area are: $a_x = 0.1$, $a_y = 0.08$, $x_0^{\inf} = L_0/2$, $y_0^{\inf} = L_0/2 - 0.15$, $x_0^{\sup} = L_0/2$, $y_0^{\sup} = L_0/2 + 0.15$, $k = 4.6$, $g_{\max} = 11.7\left[\text{rad nm}^{-2}\right]$.

5.1 Comments of the numerical simulation

Fig. 1(a) represents the initial inhomogeneities described by the scalar dislocation density $\rho = \sqrt{\alpha_{13}^2 + \alpha_{23}^2}$. The initial heterogeneities in the distribution of the tensorial dislocation density can be characterized by the Burgers vectors identified by $\mathbf{b}^0 = \alpha_{13}^0\mathbf{e}_1 + \alpha_{23}^0\mathbf{e}_2$ with $\alpha_{13}^0 = \left(\text{curl}\,\mathbf{H}_0^p\right)_{13}, \alpha_{23}^0 = \left(\text{curl}\,\mathbf{H}_0^p\right)_{23}$, and they are plotted in Fig. 8. Such orientation of Burgers vectors induces a dipole of disclinations in the deformation process which is defined by the disclination density $|\theta_{33}| = \left|(\text{curl}\boldsymbol{\Lambda})_{33}\right|$ (see Fig. 1(b)). The disclinations dipole area is very small in the immediately initial plastic state of the deformation. The dipole area is extending during the deformation process (see Fig. 2(b)). The initial plastic distortion component distributed on the sheet is represented in Fig. 1(c).

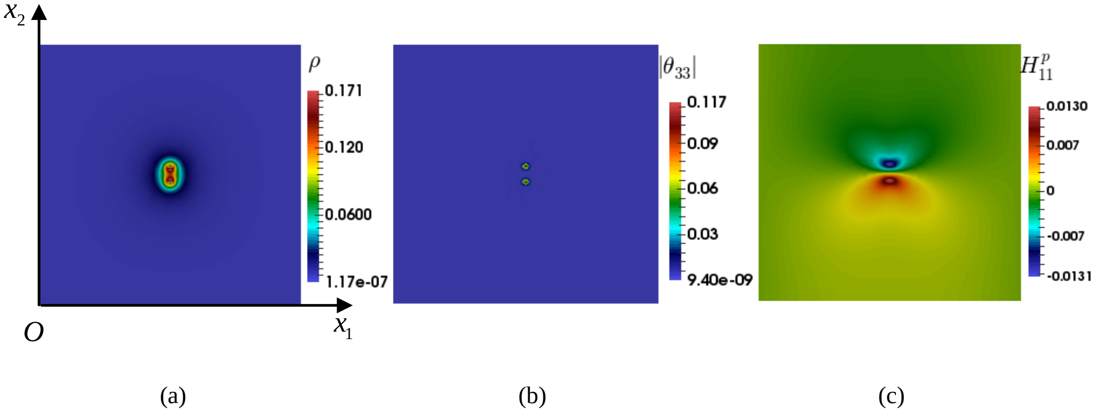

Fig.1 (a) The distribution of the dislocations density on the sheet (measured in nm^{-1}) at the initial plastic deformation that corresponds to $\varepsilon_{11} = 0.1\%$. (b) The occurrence of disclinations dipole in the immediately initial plastic state of the deformation. (c) The distribution of the plastic tensor component H_{11}^p on the sheet at the initial plastic state.

One can observe two adjacent areas of opposing signs in the distribution of plastic distortion component H_{11}^p (see Fig. 1(c)) and in the distribution of the stress tensor component T_{11} (see Fig. 3(c)). At the border line of the two adjacent areas, the shear component of the plastic distortion and of the Cauchy stress tensor takes extreme values (see Figs. 5(a,b)).

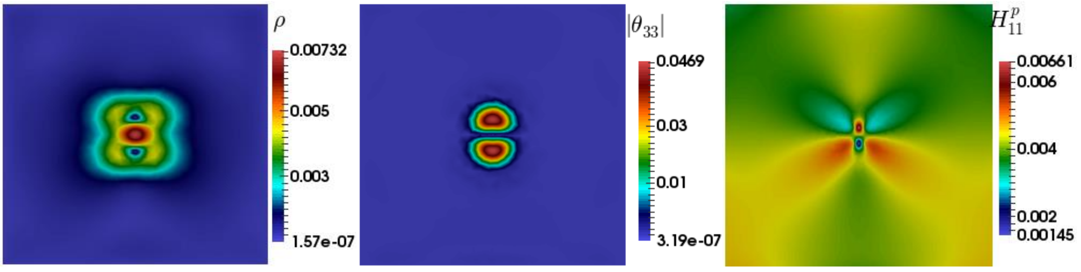

(a) (b) (c)

Fig. 2 The distribution on the sheet of (a) the dislocation density (in nm^{-1}), (b) the disclination density (in nm^{-2}) and (c) the plastic component H_{11}^{p}, at the total deformation of $\varepsilon_{11} = 1\%$

The distributions on the sheet of the disclination tensor components Λ_{31}, Λ_{32} in the immediately initial plastic state of the deformation and at the total deformation of 1% are represented in Figs. 3(a,b) and Figs. 4(a,b).

Due to the diffusion effect the disclination components are extending on the entire sheet. The values increase during the deformation process until the total deformation of 0.3%, after which their values decrease until the total deformation of 2%. One can see this effect also in the diagram plotted in Fig. 7(b).

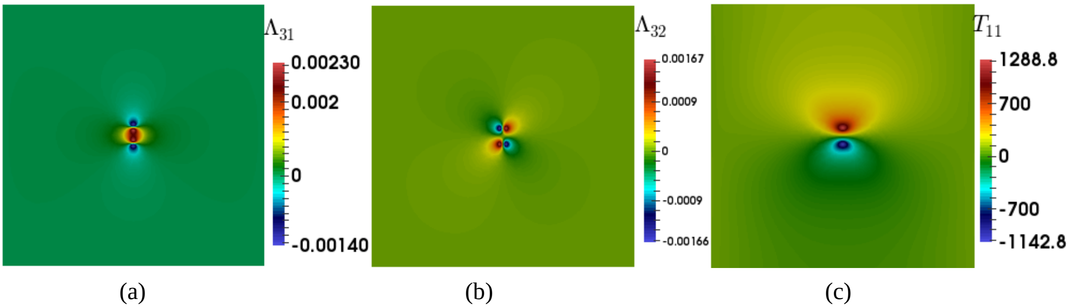

(a) (b) (c)

Fig. 3 The distribution on the sheet of the disclination tensor components (a) Λ_{31}, (b) Λ_{32} in the immediately initial plastic state of the deformation. (c) The distribution on the sheet the tensor stress component T_{11} at the initial state of plastic deformation.

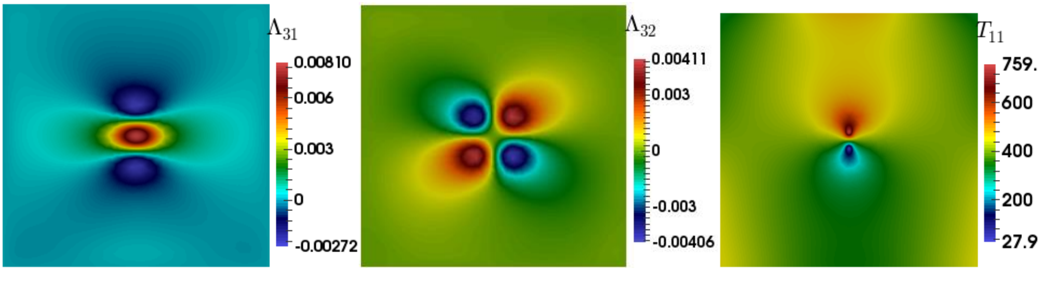

(a) (b) (c)

Fig. 4 The distribution on the sheet of (a) the disclination tensor components Λ_{31}, (b) Λ_{32} and (c) the tensor stress component T_{11}, at the total deformation of $\varepsilon_{11} = 1\%$.

With increasing strain the axial stress and axial plastic distortion components are strongly influenced. The significant variations for the axial stress and axial plastic distortion have been numerically emphasized: the tensile behavior becomes dominant (no significant changes in shear component are observed).

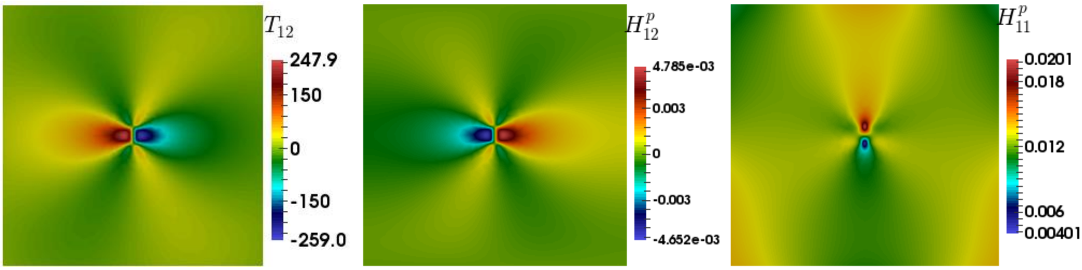

(a) (b) (c)

Fig. 5 The distribution on the sheet at the initial plastic state that corresponds to $\varepsilon_{11} = 0.1\%$, for:
(a) the shear stress component T_{12}; (b) the shear plastic component H_{12}^p.
(c) The distribution on the sheet of the plastic distortion component H_{11}^p at the total strain of $\varepsilon_{11} = 2\%$.

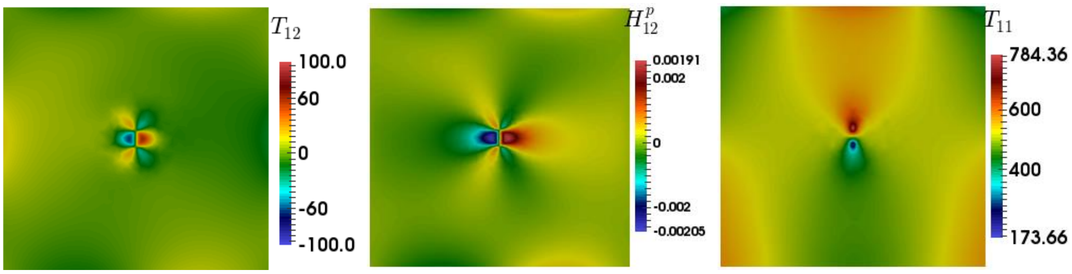

(a) (b) (c)

Fig. 6 The distribution on the sheet at the total strain to $\varepsilon_{11} = 1\%$, for:
(a) the shear stress component T_{12}; (b) the shear plastic component H_{12}^p.
(c) The distribution of the stress tensor component T_{11} at the total strain of $\varepsilon_{11} = 2\%$.

In the deformation process T_{11} tends to become homogeneous on the entire plate (the difference between the extreme values is decreasing) (see Fig. 4(c) and Fig. 6(c)). The H_{11}^p component has a tendency to change its aspect Fig. 2(c). In the central zone two opposing sign areas appear. This effect is due to the influence of the stress (see Fig. 3(c)). At the total deformation of 2%, the aspect of the plastic distortion component H_{11}^p in the sheet is entirely similar to the stress tensor component T_{11} (compare Fig. 4(c) to Fig. 5(c)). The plastic deformation tends to homogenize until the total deformation of about 1.8%, after which

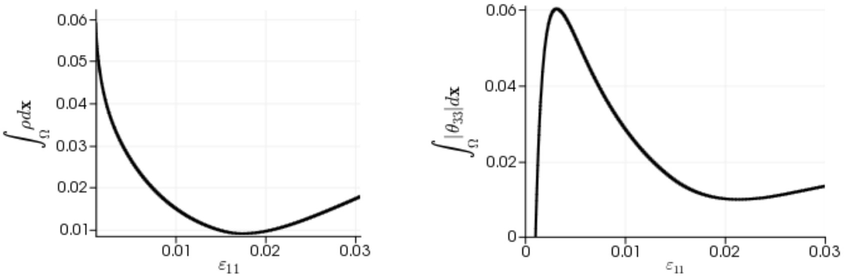

(a) (b)

Fig. 7. (a) Time variation of the average dislocation density versus total strain.
(b) Time variation of the average disclination density versus total strain.

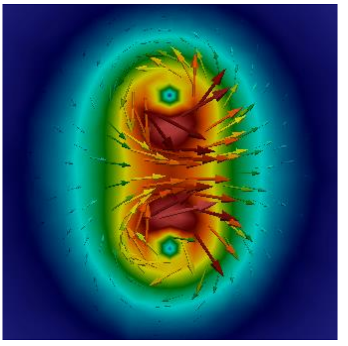

Fig. 8 The distribution of the Burgers vectors in the central zone of the sheet at the initial plastic deformation state.

H_{11}^{p} tends to become more inhomogeneous (see Fig. 5(c)). One can observe this effect in Fig. 7(a).

6. CONCLUSIONS

We used an elasto-plastic constitutive model, in order to describe the behaviour of crystalline materials, with microstructural defects such as dislocations and disclinations.

In the case of small distortions, the equations describing the evolution for the plastic distortion and the disclination tensor were considered to be non-local diffusion-like evolution equations. These equations can describe the interaction between dislocations and disclinations.

The initial and boundary value problem concerning the tensile test of a rectangular sheet was formulated. This problem was solved numerically, using the FEM method. For the initial state we assumed the existence of defects inside the microstructure, modelled by the dislocation tensor. We observed the occurrence of a dipole of disclinations starting from a punctual central zone and the diffusion in time of the defects.

From this numerical experiment we observed that the plastic deformation covered the entire plate, comparing to the case described in paper [10].

ACKNOWLEDGEMENTS

Raisa Pașcan was supported by the strategic grant POSDRU/159/1.5/S/137750, “Project Doctoral and Postdoctoral programs support for increased competitiveness in Exact Sciences research” cofinanced by the European Social Found within the Sectorial Operational Program Human Resources Development 2007-2013.

Sanda Cleja-Țigoiu was supported by the Romanian National Authority for Scientific Research (CNCS- UEFISCDI; project number PN II-ID-PCE-2011-3-0521).

REFERENCES

[1] A. Acharya, New inroads in an old subject: Plasticity, from around the atomic to the macroscopic scale, *J. Mech. Phys. Solids*, **58**, 766 - 778, 2010.

[2] B. Beausir, C. Fressengeas, Disclination densities from EBSD orientation mapping, *Int. J. Solids Struct.*, **50**, 137 - 146, 2013.

[3] B. A. Bilby, *Continuous distribution of dislocations*, In: Sneddon I N, Hill R (eds) Progress in Solid Mechanics, North-Holland, Amsterdam, 329 - 398, 1960.

[4] S. Cleja-Ţigoiu, Material forces in finite elasto-plasticity with continuously distributed dislocations, *Int. J. Fracture*, **147**, 67 - 81, 2007.

[5] S. Cleja-Ţigoiu, Elasto-plastic materials with lattice defects modeled by second order deformations with non-zero curvature, *Int. J. Fracture*, **166**, 61 - 75, 2010.

[6] S. Cleja-Ţigoiu, Non-local elasto-viscoplastic models with dislocations in finite elasto-plasticity. Part I: Constitutive framework, *Math. Mech. Solids*, **18**, 349 - 372, 2013.

[7] S. Cleja-Ţigoiu, R. Paşcan, Influence of Dislocations on the Deformability of Metallic Sheets, *Key Engineering Materials, Trans Tech Publications*, **554-557**, 99-109, 2013.

[8] S. Cleja-Ţigoiu, R. Paşcan, Slip systems and flow patterns in viscoplastic metallic sheets with dislocations, *Int. J. Plasticity*, **61**, 64 - 93, 2014.

[9] S. Cleja - Ţigoiu, R. Paşcan, Non-local elasto-viscoplastic models with dislocations in finite elasto-plasticity. Part II: Influence of dislocation density, *Math. Mech. Solids,* **18: 4,** 373-396, 2013.

[10] S. Cleja-Ţigoiu, R. Paşcan, V. Ţigoiu, Elastoplastic models with continuously distributed defects: dislocations and disclinations, for finite and small strains, *Int. J. Plasticity*, submitted.

[11] C. Fressengeas, V. Taupin, L. Capolungo, An elasto-plastic theory of dislocation and disclination fields, *Int. J. Solids Sruct.* **48**, 3499-3509, 2011.

[12] M. E. Gurtin, On a framework for small-deformation viscoplasticity: free energy, microforces, strain gradien, *Int. J. Plasticity*, 47-90, 2003.

[13] M. E. Gurtin, E. Fried, L. Anand, *The Mechanics and Thermodynamics of Continua*, Cambridge University Press, 2010.

[14] F. Hecht, S. Auliac, O. Pironneau, J. Morice, A. Le Hyaric, K. Ohtsuka, FreeFem++, http://www.freefem.org/ff++/ftp/freefem++doc.pdf, (Accessed 20 may, 2014).

[15] V. Taupin, L. Capolungo, C. Fressengeas, C., Das, M. Upadhyay, Grain boundary modeling using an elasto-plastic theory of dislocation and disclination fields, *J. Mech. Phys. Solids*, **61**, 370- 384, 2013.

[16] M. Zlámal, Finite element methods for nonlinear parabolic equations, *RAIRO Analyse numérique*, **11**, 93 - 107, 1977.